

Electronic Supplementary Information for

# From Blue to White to Yellow Emitter: A Hexanuclear Copper Iodide Nanocluster

Ke Xu, Bu-Lin Chen, Rui Zhang, Li Liu\*, Xin-Xin Zhong\*, Lei Wang\*, Feng-Yan Li\*, Guang-Hua

Li, Khalid A. Alamry, Fa-Bao Li, Wai-Yeung Wong\*, Hai-Mei Qin

## Contents

### Experimental Details

#### 1. NMR Experiments

**Fig. S1.**  $^1\text{H}$  NMR spectrum of ppda in  $\text{CDCl}_3$ .

**Fig. S2.**  $^1\text{H}$  NMR spectrum of  $[\text{Cu}_6\text{I}_6(\text{ppda})_2]$  in  $\text{CDCl}_3$ .

**Fig. S3.**  $^{13}\text{C}$  NMR spectrum of ppda in  $d_6\text{-DMSO}$ .

**Fig. S4.**  $^{31}\text{P}$  NMR spectrum of ppda in  $\text{CDCl}_3$ .

**Fig. S5.**  $^{31}\text{P}$  NMR spectrum of  $[\text{Cu}_6\text{I}_6(\text{ppda})_2]$  in  $\text{CDCl}_3$ .

#### 2. Molecular structures

**Fig. S6.** ORTEP diagram of complex  $[\text{Cu}_6\text{I}_6(\text{ppda})_2]$ .

**Fig. S7.** 2-D sheet in the  $ab$  plane and C–H $\cdots\pi$  interactions in  $[\text{Cu}_6\text{I}_6(\text{ppda})_2]$ .

**Fig. S8.** PXRD profiles of powder and film samples of  $[\text{Cu}_6\text{I}_6(\text{ppda})_2]$  at 297 K.

#### 3. Photophysical properties

**Fig. S9.** The concentration dependence of the UV-Vis absorption spectra of complex  $[\text{Cu}_6\text{I}_6(\text{ppda})_2]$  in  $\text{CH}_3\text{CN}$ .

**Fig. S10.** Time profiles of luminescence decay and exponential fit spectrum of  $[\text{Cu}_6\text{I}_6(\text{ppda})_2]$  at 297 K with  $\lambda_{\text{em}} = 476$  nm in crystal state.

**Fig. S11.** Time profiles of luminescence decay and exponential fit spectrum of  $[\text{Cu}_6\text{I}_6(\text{ppda})_2]$  at 297 K with  $\lambda_{\text{em}} = 716$  nm in crystal state.

**Fig. S12.** Time profiles of luminescence decay and exponential fit spectrum of  $[\text{Cu}_6\text{I}_6(\text{ppda})_2]$  at 77 K with  $\lambda_{\text{em}} = 470$  nm in crystal state.

**Fig. S13.** Time profiles of luminescence decay and exponential fit spectrum of

$[\text{Cu}_6\text{I}_6(\text{ppda})_2]$  at 297 K with  $\lambda_{\text{em}} = 535$  nm in powder state.

**Fig. S14.** Time profiles of luminescence decay and exponential fit spectrum of  $[\text{Cu}_6\text{I}_6(\text{ppda})_2]$  at 297 K with  $\lambda_{\text{em}} = 470$  nm in powder state.

**Fig. S15.** Excitation spectra of ligand ppda and complex  $[\text{Cu}_6\text{I}_6(\text{ppda})_2]$  in crystal and powder states at 297 K.

**Fig. S16.** Normalized emission spectra of ligand ppda and complex  $[\text{Cu}_6\text{I}_6(\text{ppda})_2]$  in powder state at 297 K ( $\lambda_{\text{ex}} = 370$  nm).

**Fig. S17.** Normalized emission spectra of  $[\text{Cu}_6\text{I}_6(\text{ppda})_2]$  in powder state at 297 K ( $\lambda_{\text{ex}} = 350$  nm) and 77 K ( $\lambda_{\text{ex}} = 320$  nm).

#### 4. Computational details

**Fig. S18.** The absorption spectrum of complex  $[\text{Cu}_6\text{I}_6(\text{ppda})_2]$  in  $\text{CH}_3\text{CN}$ .

**Fig. S19.** Contour plots of frontier molecular orbitals of complex  $[\text{Cu}_6\text{I}_6(\text{ppda})_2]$  in  $\text{CH}_3\text{CN}$ .

**Fig. S20.** SEM-EDS for the  $\text{Cu}_6\text{I}_6$  cluster (a) before and (b) after the photocatalysis.

**Table S1.** Selected bond lengths ( $\text{\AA}$ ) and angles ( $^\circ$ ) in the optimized  $S_0$ , and  $S_1$  geometries for complex  $[\text{Cu}_6\text{I}_6(\text{ppda})_2]$ .

**Table S2.** Computed excitation states for complex  $[\text{Cu}_6\text{I}_6(\text{ppda})_2]$  in  $\text{CH}_3\text{CN}$ .

**Table S3.** Calculated photophysical data of  $[\text{Cu}_6\text{I}_6(\text{ppda})_2]$  from the crystal data.

## Experimental Details

### 1. NMR Experiments

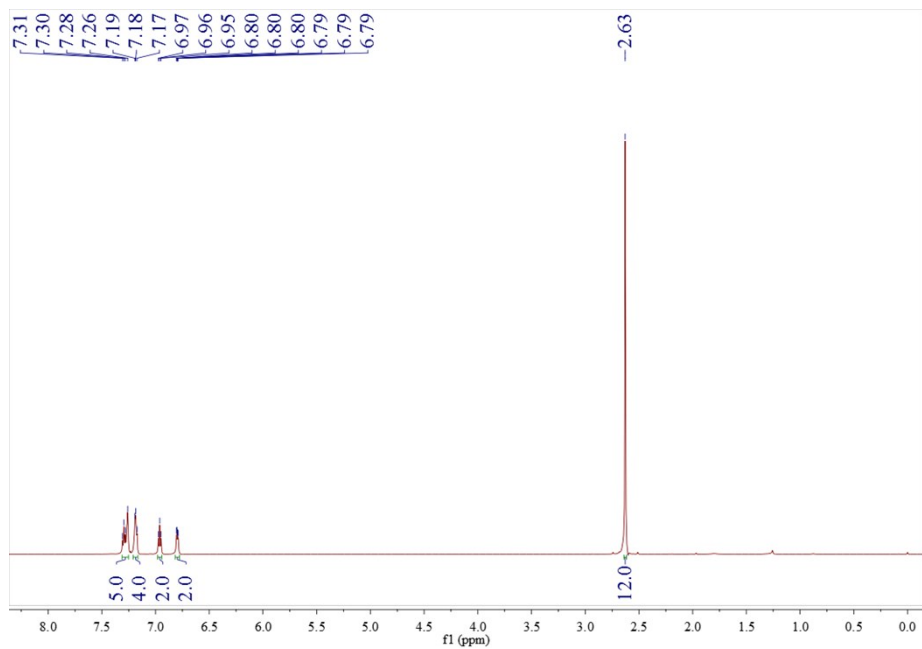


**Fig. S1.** <sup>1</sup>H NMR spectrum of ppda in CDCl<sub>3</sub>.

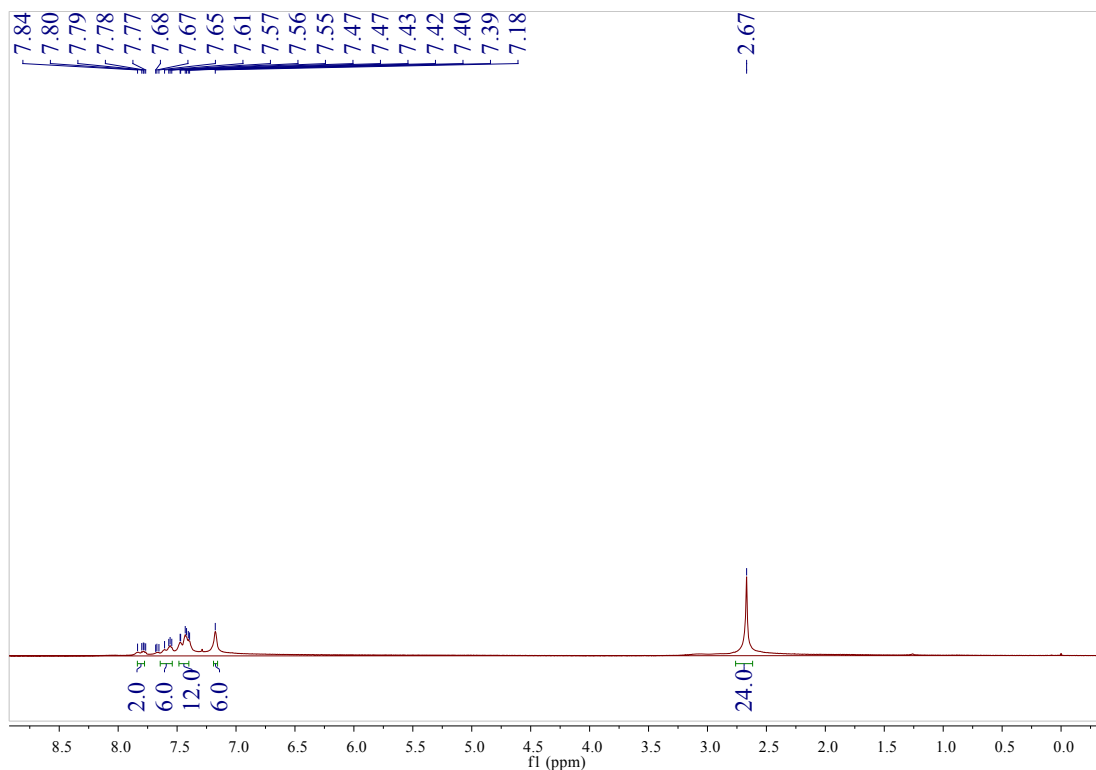


**Fig. S2.** <sup>1</sup>H NMR spectrum of Cu<sub>6</sub>I<sub>6</sub>(ppda)<sub>2</sub> in CDCl<sub>3</sub>.

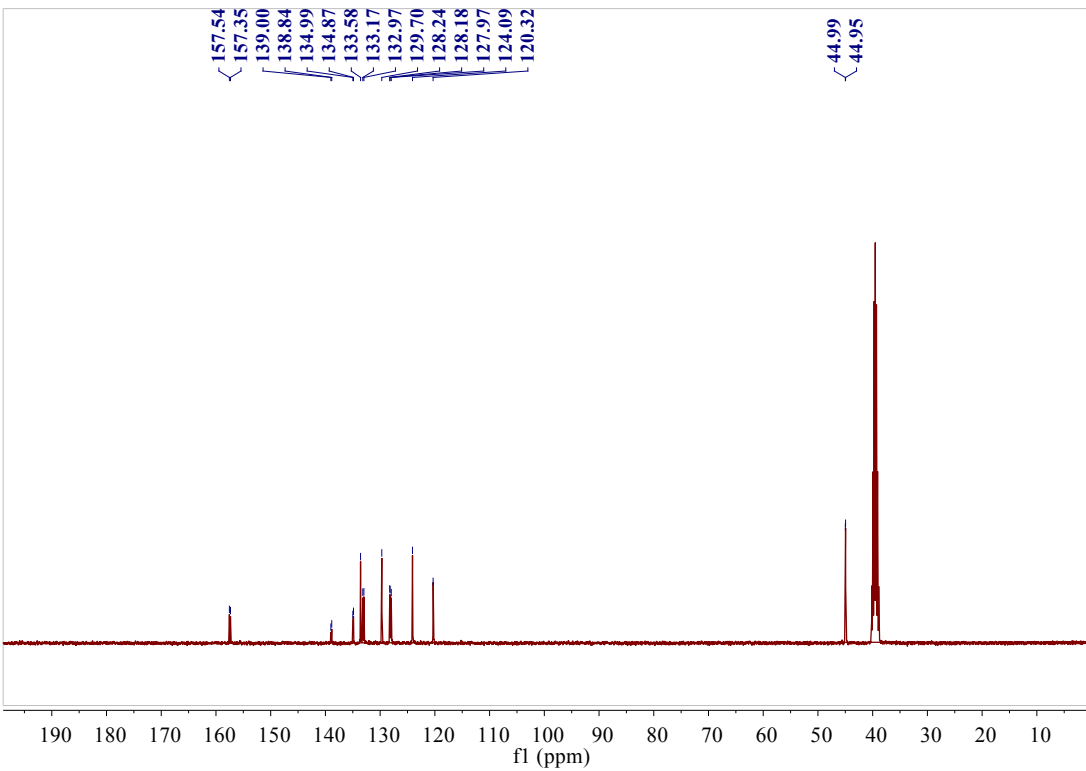


**Fig. S3.**  $^{13}\text{C}$  NMR spectrum of ppda in  $d_6$ -DMSO.

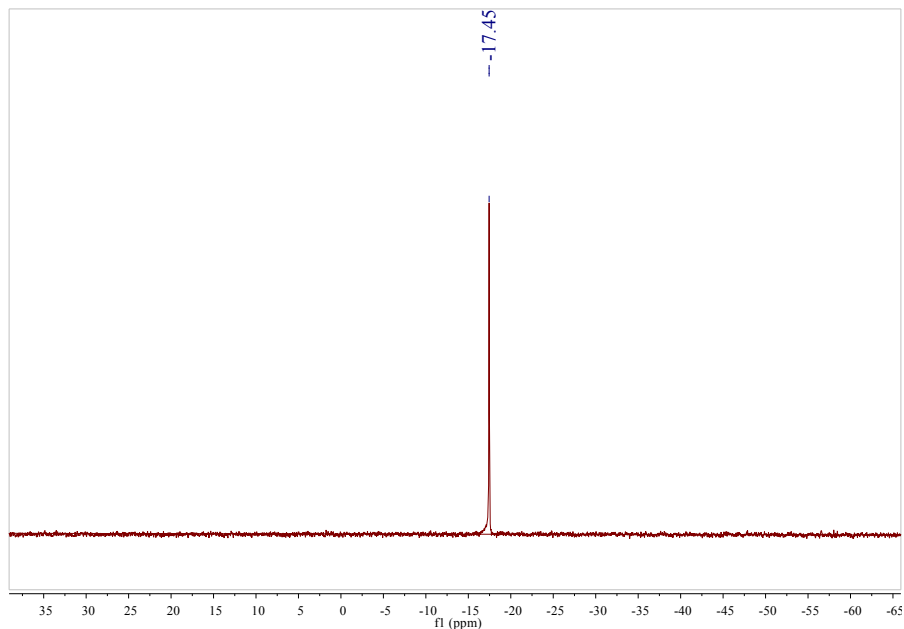


**Fig. S4.**  $^{31}\text{P}$  NMR spectrum of ppda in  $\text{CDCl}_3$ .

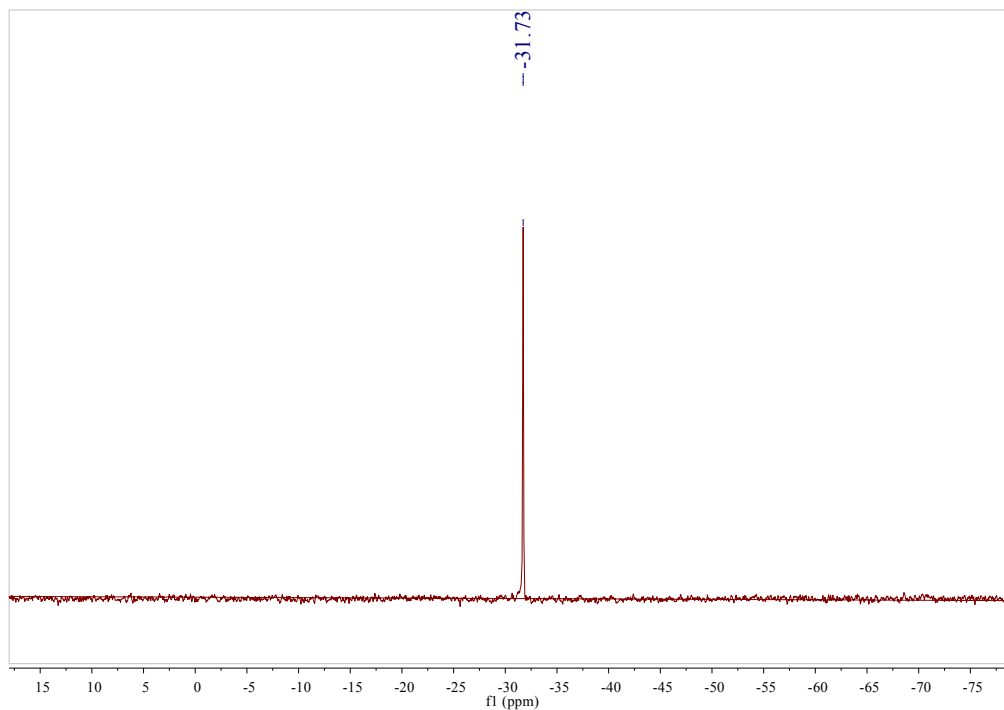


**Fig. S5.**  $^{31}\text{P}$  NMR spectrum of  $\text{Cu}_6\text{I}_6(\text{ppda})_2$  in  $\text{CDCl}_3$ .

## 2. Molecular structures

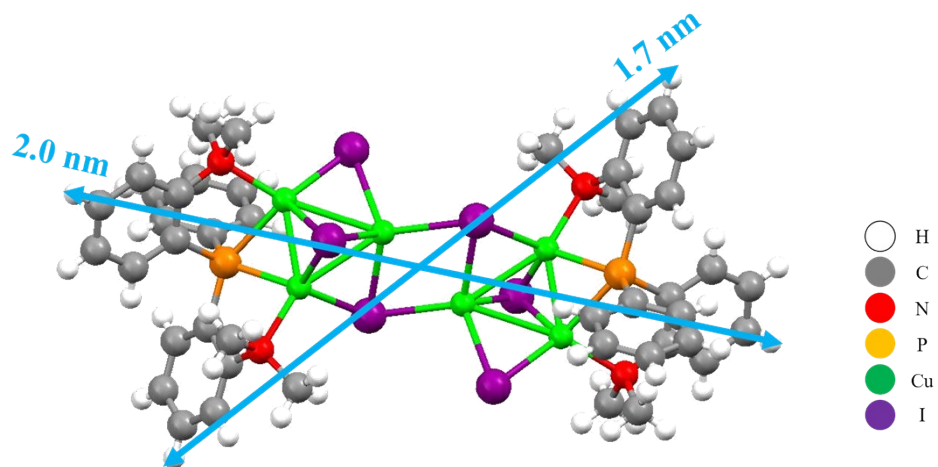


**Fig. S6.** ORTEP diagram of complex  $[\text{Cu}_6\text{I}_6(\text{ppda})_2]$ .

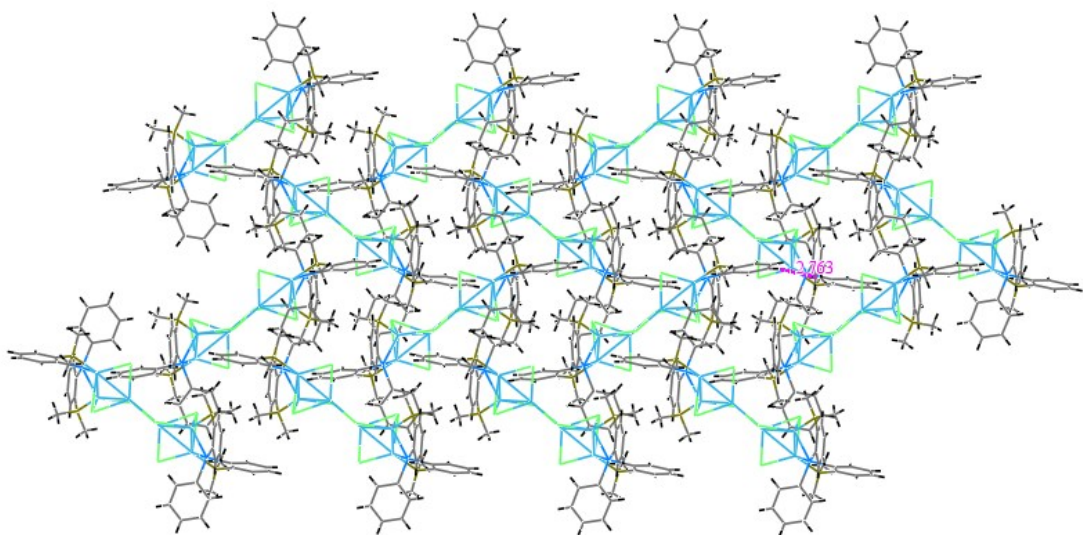


**Fig. S7.** 2-D sheet in the *ab* plane and C–H $\cdots$  $\pi$  interactions in  $[\text{Cu}_6\text{I}_6(\text{ppda})_2]$ .

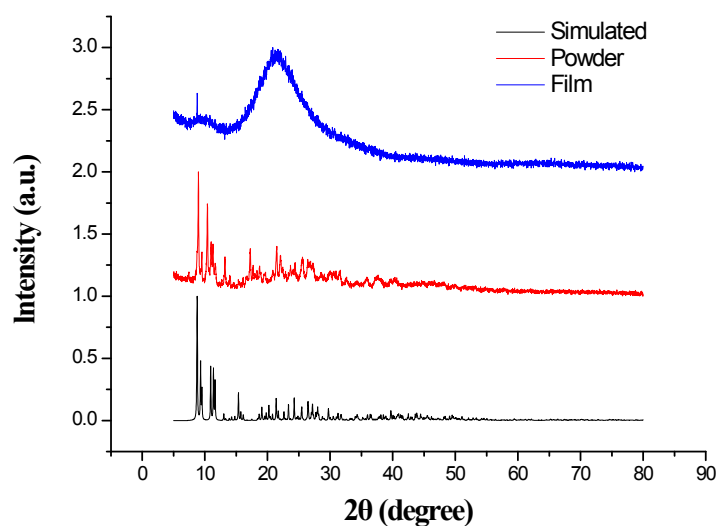


**Fig. S8.** PXRD profiles of powder and film samples of  $[\text{Cu}_6\text{I}_6(\text{ppda})_2]$  at 297 K.

### 3. Photophysical properties

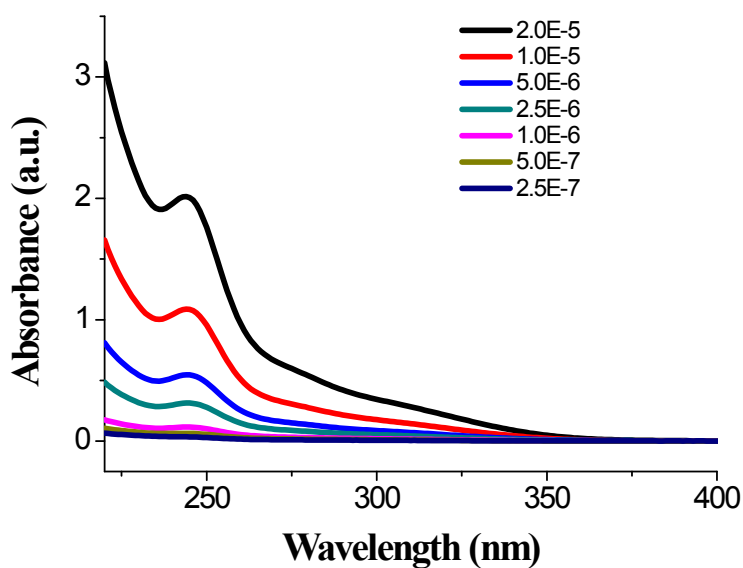


**Fig. S9.** The concentration dependence of the UV-Vis absorption spectra of complex  $[\text{Cu}_6\text{I}_6(\text{ppda})_2]$  in  $\text{CH}_3\text{CN}$ .

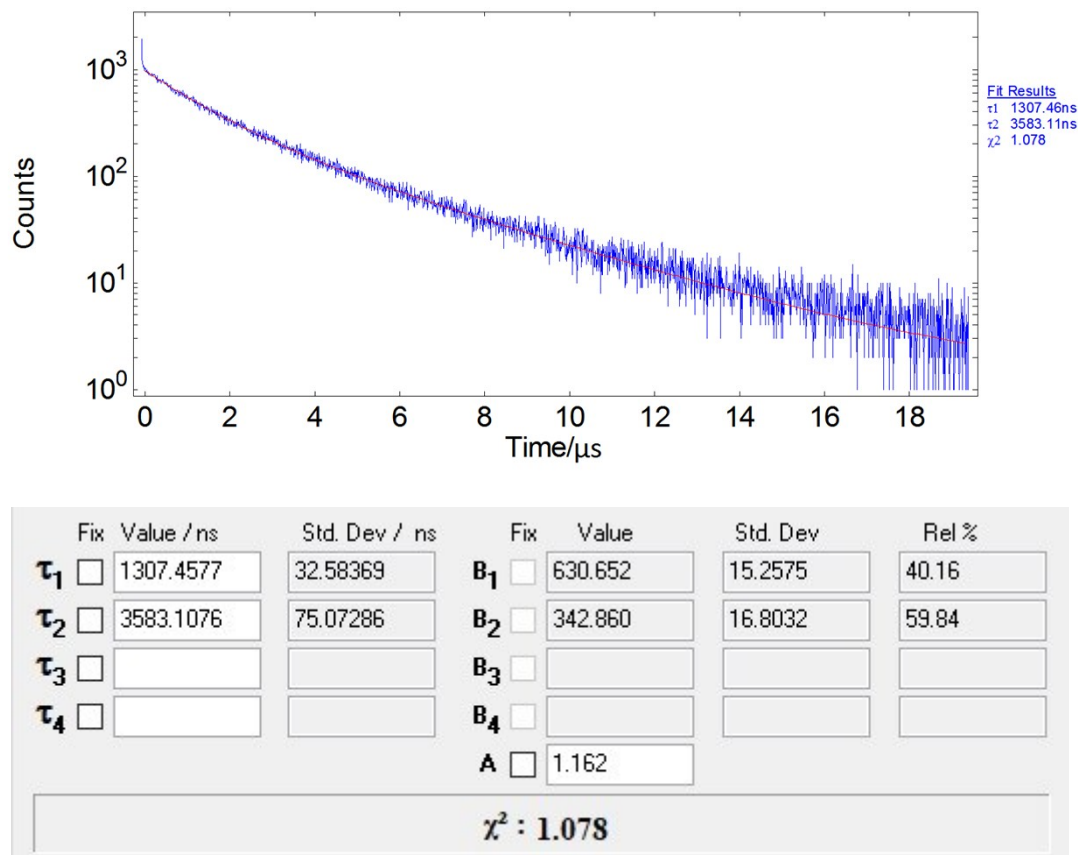


**Fig. S10.** Time profiles of luminescence decay and exponential fit spectrum of  $[\text{Cu}_6\text{I}_6(\text{ppda})_2]$  at 297 K with  $\lambda_{\text{em}} = 476 \text{ nm}$  in crystal state.

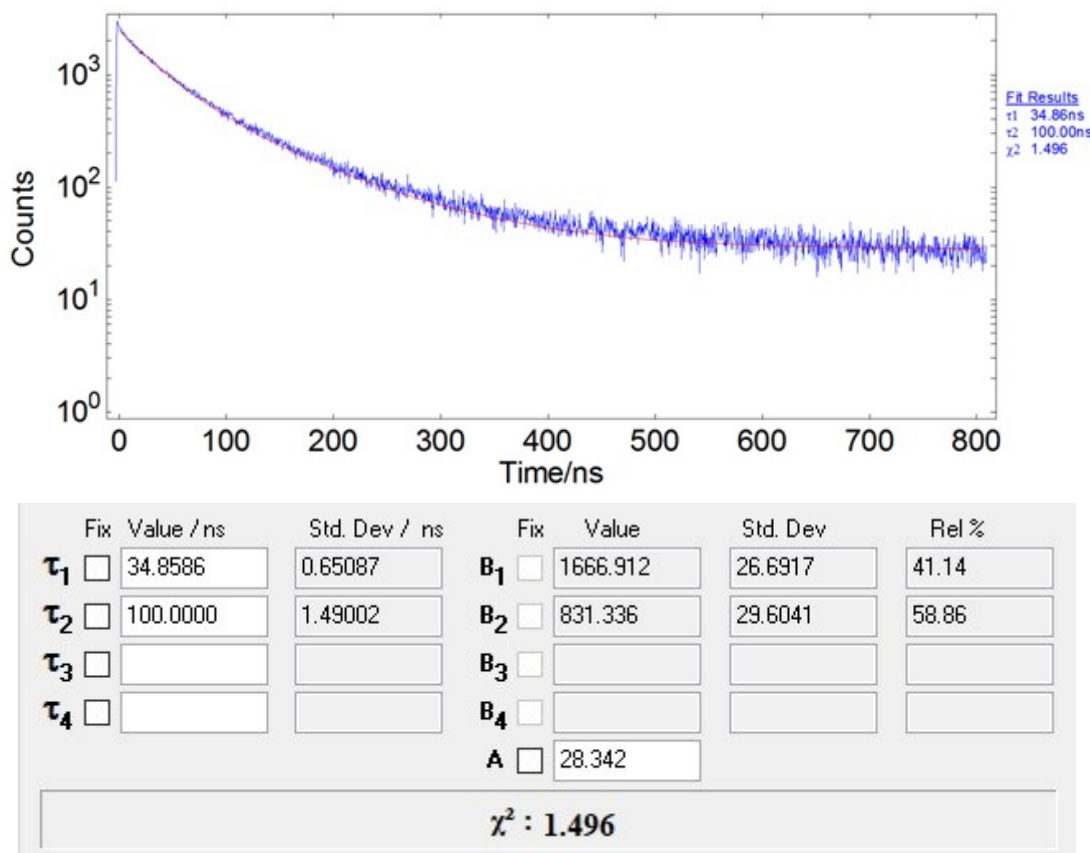
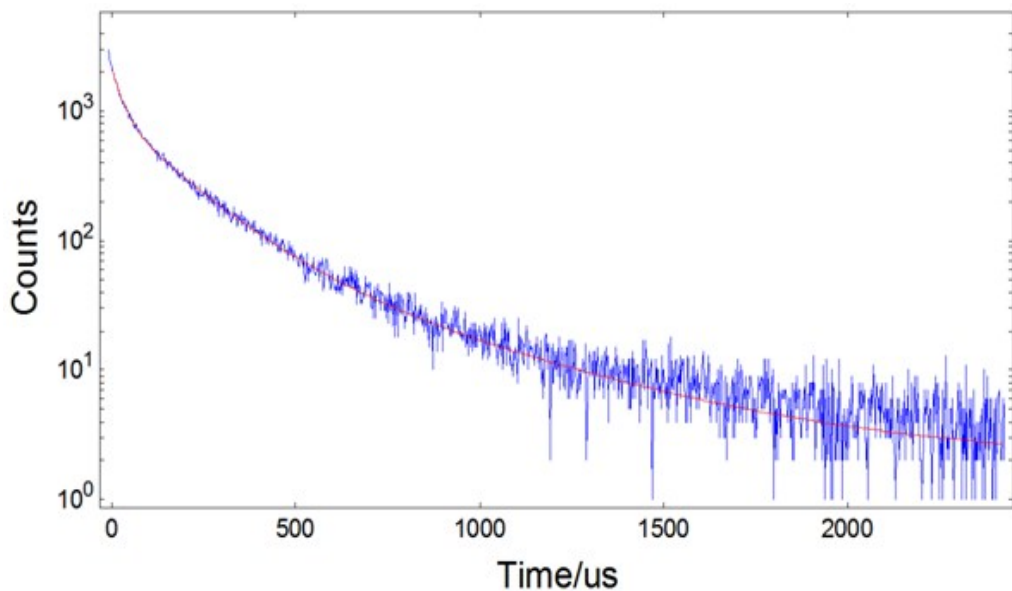


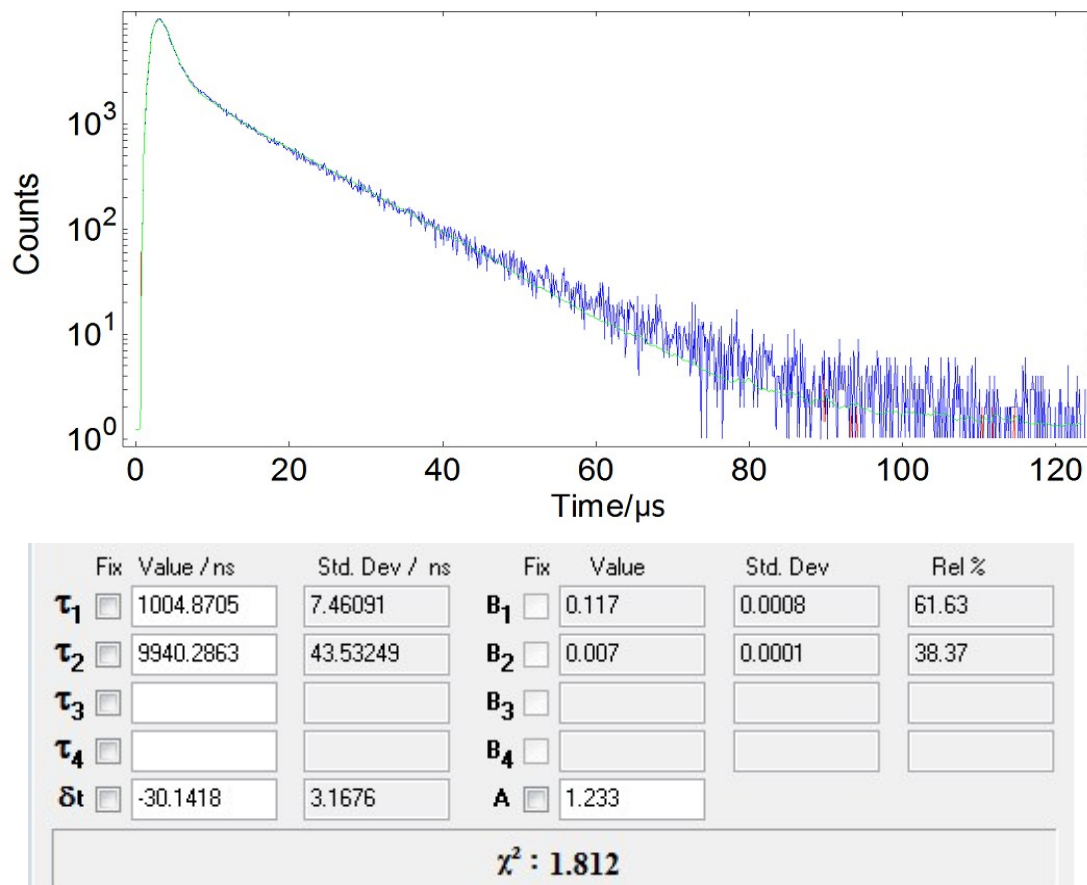
**Fig. S11.** Time profiles of luminescence decay and exponential fit spectrum of  $[\text{Cu}_6\text{I}_6(\text{ppda})_2]$  at 297 K with  $\lambda_{\text{em}} = 716$  nm in crystal state.



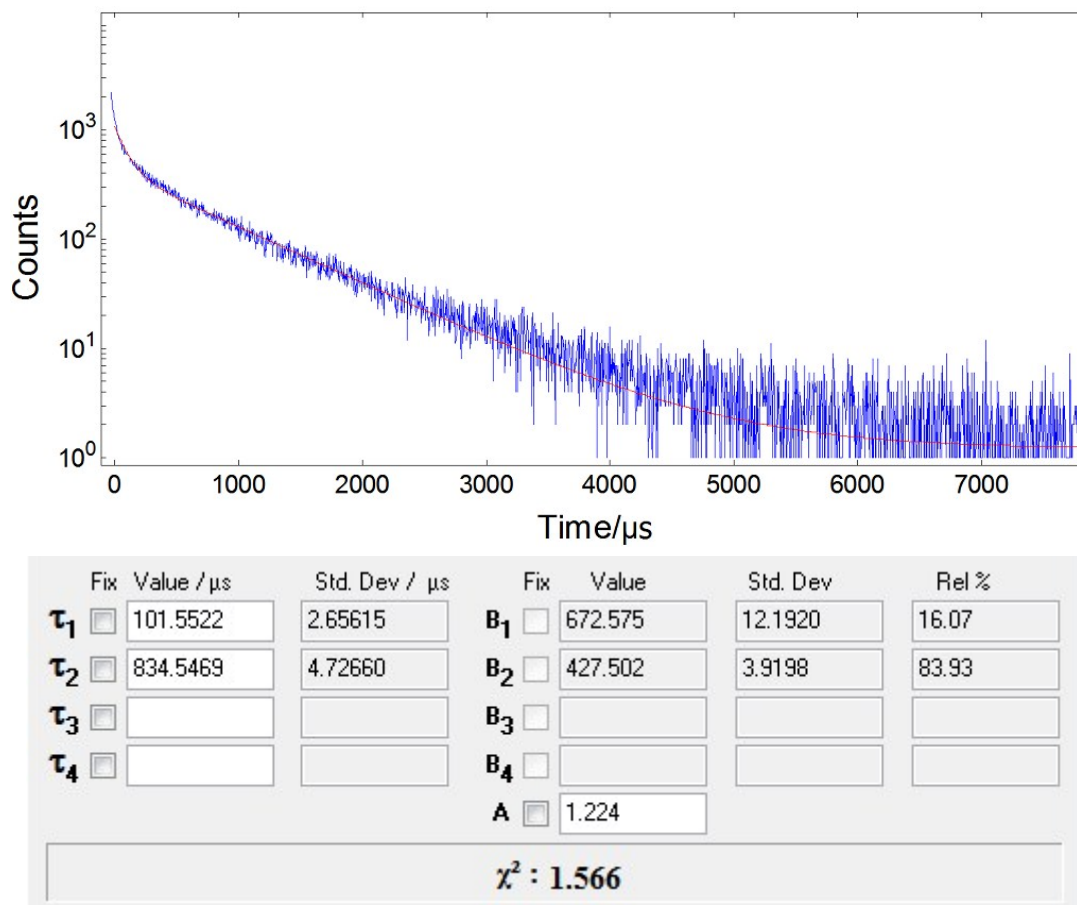
Value	Std Dev	Value	Std Dev	Rel %
T1 2.828E-5	1.053E-6	B1 1.300E+3	2.735E+1	16.84

T2	1.573E-4	5.384E-6	B2	8.150E+2	1.627E+1	58.72
T3	4.767E-4	3.292E-5	B3	1.119E+2	1.732E+1	24.43
			Chisq	1.295E+0	A	2.011E+0

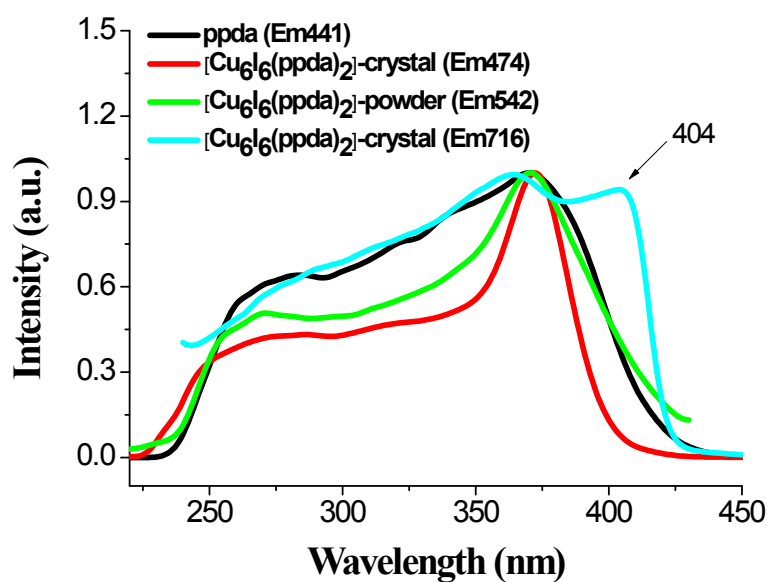
**Fig. S12.** Time profiles of luminescence decay and exponential fit spectrum of  $[\text{Cu}_6\text{I}_6(\text{ppda})_2]$  at 77 K with  $\lambda_{\text{em}} = 470$  nm in crystal state.



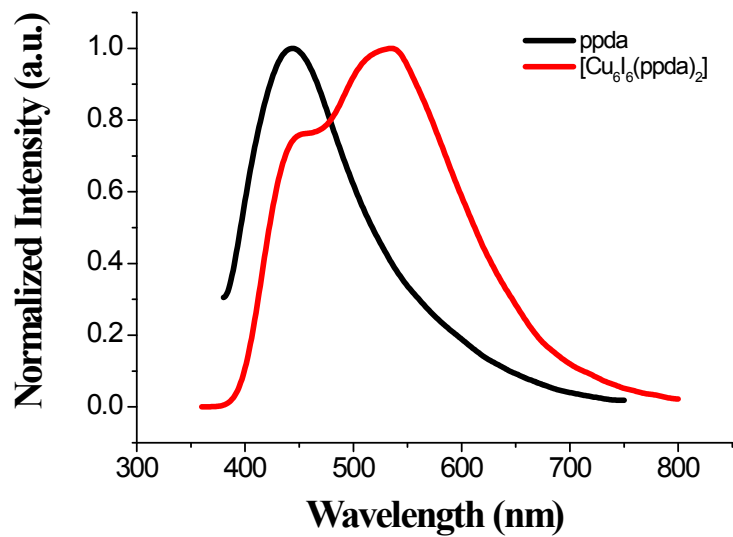
**Fig. S13.** Time profiles of luminescence decay and exponential fit spectrum of  $[\text{Cu}_6\text{I}_6(\text{ppda})_2]$  at 297 K with  $\lambda_{\text{em}} = 535$  nm in powder state.



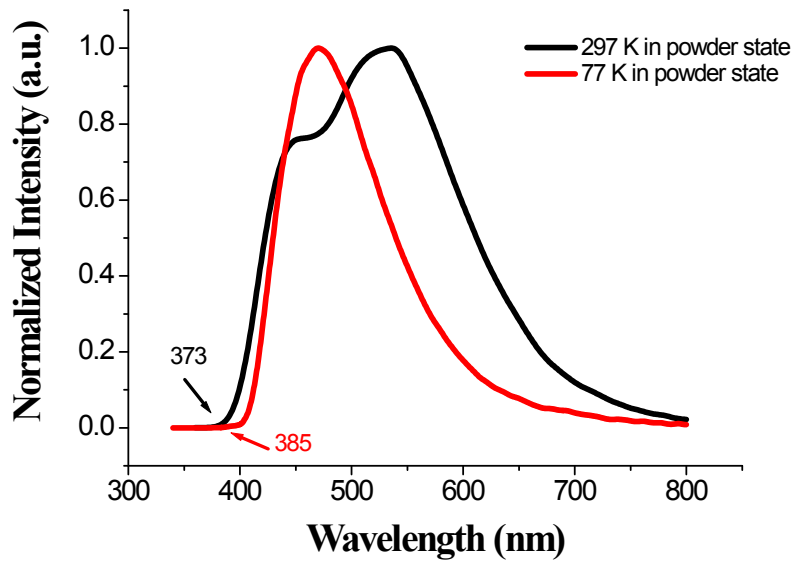
**Fig. S14.** Time profiles of luminescence decay and exponential fit spectrum of  $[\text{Cu}_6\text{I}_6(\text{ppda})_2]$  at 77 K with  $\lambda_{\text{em}} = 470$  nm in powder state.



**Fig. S15.** Excitation spectra of ligand ppda and complex  $[\text{Cu}_6\text{I}_6(\text{ppda})_2]$  in crystal and powder states at 297 K.

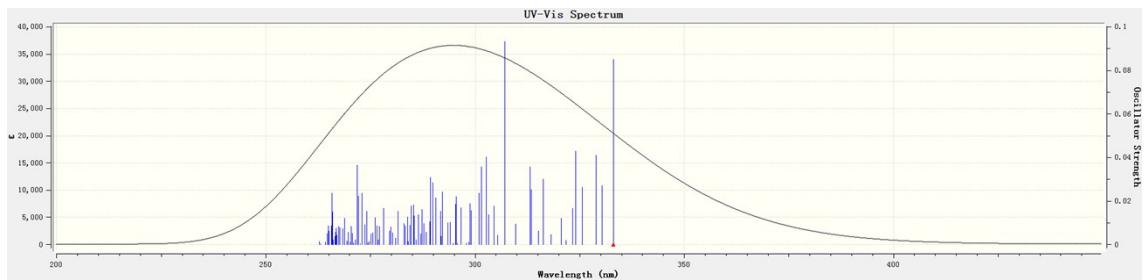


**Fig. S16.** Normalized emission spectra of ligand ppda and complex  $[\text{Cu}_6\text{I}_6(\text{ppda})_2]$  in powder state at 297 K ( $\lambda_{\text{ex}} = 370$  nm).

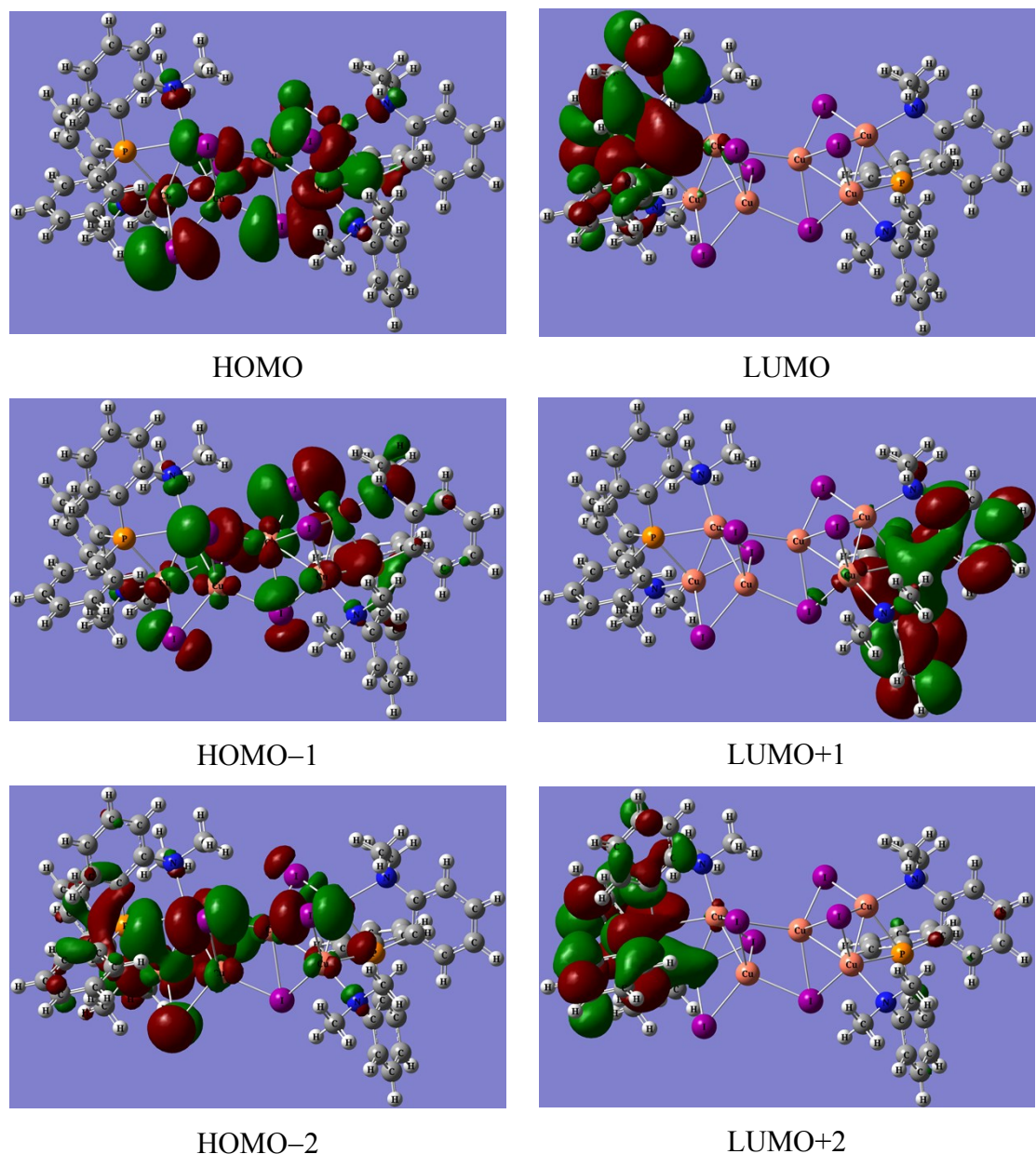


**Fig. S17.** Normalized emission spectra of  $[\text{Cu}_6\text{I}_6(\text{ppda})_2]$  in powder state at 297 K ( $\lambda_{\text{ex}} = 350$  nm) and 77 K ( $\lambda_{\text{ex}} = 320$  nm).

#### 4. Computational details



**Fig. S18.** The absorption spectrum of complex  $[\text{Cu}_6\text{I}_6(\text{ppda})_2]$  in  $\text{CH}_3\text{CN}$ .



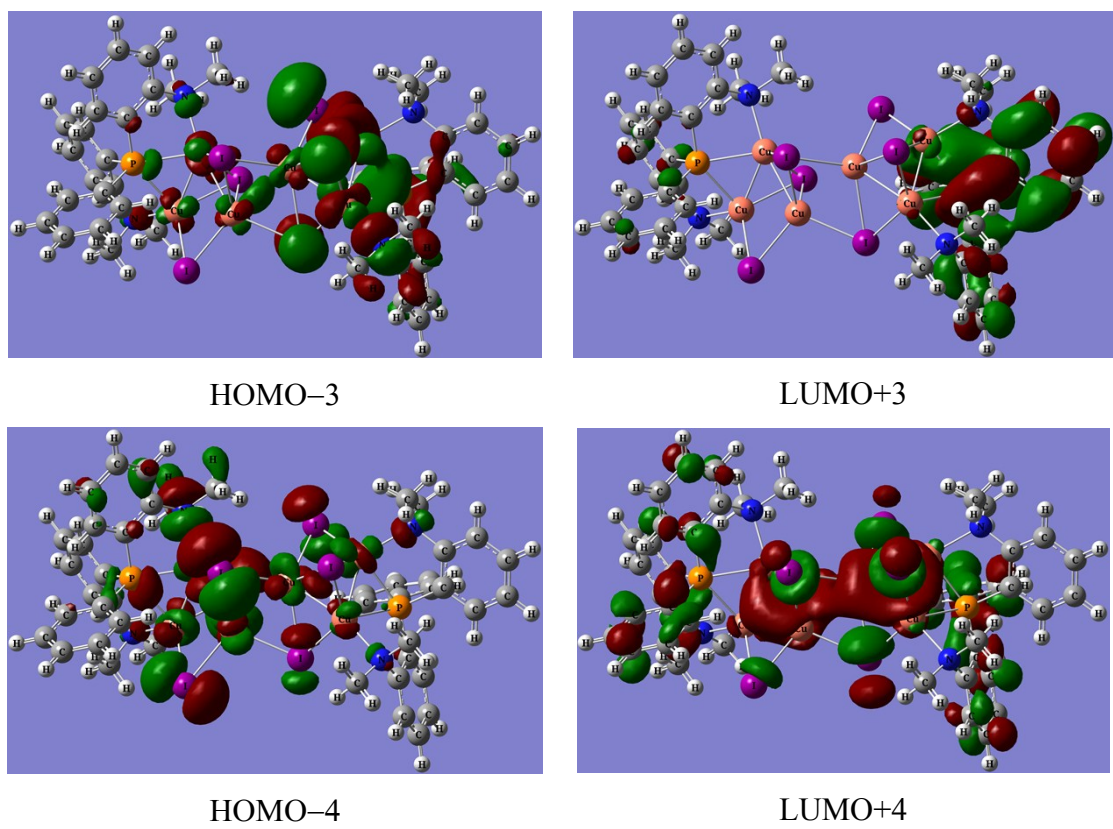


**Fig. S19.** Contour plots of frontier molecular orbitals of complex  $[\text{Cu}_6\text{I}_6(\text{ppda})_2]$  in  $\text{CH}_3\text{CN}$ .

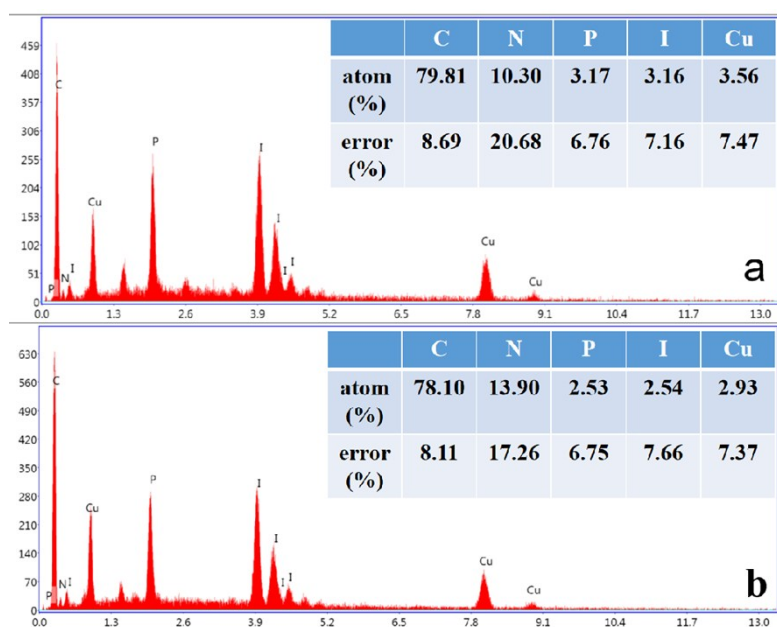


**Fig. S20.** SEM-EDS for the  $\text{Cu}_6\text{I}_6$  cluster (a) before and (b) after the photocatalysis.

**Table S1.** Selected bond lengths ( $\text{\AA}$ ) and angles ( $^\circ$ ) in the optimized  $S_0$  and  $S_1$  geometries for complex  $[\text{Cu}_6\text{I}_6(\text{ppda})_2]$ .

Complex	Geometry	
	$S_0$	$S_1$
$[\text{Cu}_6\text{I}_6(\text{ppda})_2]$		
Cu–I	2.7370, 2.6277, 2.6413, 2.6318 3.2665, 2.6656, 2.8291, 2.7151	2.8354, 2.6392, 2.6599, 2.6476 2.7818, 2.6247, 3.7673, 2.6110
Cu–P	2.5119, 2.4611	2.4254, 2.5127
Cu–N	2.17670, 2.1784	2.1582, 2.2043
Cu…Cu	2.44630, 2.6282, 2.7718	2.4684, 2.6368, 2.7618
I–Cu–I	114.91, 131.82, 98.86, 104.09 127.96, 92.81, 115.95, 108.88	110.59, 137.76, 112.73, 97.08 113.99, 110.43, 128.13, 87.30
Cu–I–Cu	54.07, 54.13, 51.51, 63.15, 57.40, 59.84, 113.29	53.27, 55.98, 60.95, 60.12, 47.12, 57.12, 104.08
I–Cu–N	112.84, 110.00, 108.62, 104.12	112.85, 108.50, 104.94, 98.65
I–Cu–P	114.05, 117.46, 115.69, 102.68	112.67, 124.51, 115.88, 101.60
P–Cu–N	83.42, 82.46	84.70, 81.98
Cu–P–Cu	58.92	59.95

**Table S2.** Computed excitation states for complex  $[\text{Cu}_6\text{I}_6(\text{ppda})_2]$  in  $\text{CH}_3\text{CN}$ .

State	$\lambda(\text{nm})/E(\text{eV})$	Configurations	$f$
1	333.1 (3.72)	H-4→L+1 (2); H-3→L+1 (4); H-1→L+1 (25); H→L+1 (62)	0.0850
3	328.9 (3.77)	H-4→L+3 (2); H-2→L (6); H-1→L+3 (27); H→L+2 (6); H→L+3 (41); H→L+4 (3)	0.0411
5	324.0 (3.83)	H-4→L (8); H-3→L (7); H-2→L (31); H-2→L+2 (6); H→L (29); H→L+2 (4); H→L+4 (3)	0.0429
15	307.1 (4.04)	H-1→L+3 (7); H-1→L+4 (7); H→L+3 (3); H→L+4 (5); H→L+5 (2); H→L+7 (5) H-6→L+2 (6); H-5→L+1 (5); H-4→L+1 (5); H-4→L+4 (26);	0.0932
19	302.6 (4.10)	H-4→L+6 (3); H-4→L+7 (6); H-3→L+4 (3); H-2→L+1 (7); H-1→L+2 (7); H-1→L+4 (6); H-1→L+7 (3)	0.0402

**Table S3.** Calculated photophysical data of  $[\text{Cu}_6\text{I}_6(\text{ppda})_2]$  from the crystal data.

Number of molecules	$\lambda(\text{nm})$	
	297 K	77 K
One	346.14	354.28
Two	436.01	437.92
three	471.01	471.01